Life history strategy varies with the strength of competition in a food-limited ungulate population

Rosemarie Kentie[1,2*], Sonya M. Clegg[1,3], Shripad Tuljapurkar[4], Jean-Michel Gaillard[5] and Tim Coulson[1]

[1] Department of Zoology, University of Oxford, Oxford OX1 3PS

[2] NIOZ Royal Netherlands Institute for Sea Research, Department of Coastal Systems, and Utrecht University, P.O. Box 59, 1790 AB Den Burg, Texel, the Netherlands

[3] Edward Grey Institute, Department of Zoology, University of Oxford OX1 3PS

[4] Department of Biology, Stanford University, Stanford, CA 94305-5020, USA

[5] UMR 5558 Biometrie et Biologie Evolutive, Batiment G. Mendel, Universite Claude Bernard Lyon 1, 43 boulevard du 11 novembre 1918, 69622 Villeurbanne Cedex, France

*Corresponding author: rosemarie.kentie@nioz.nl, +31 (0)222 369 484

Statement of authorship: TC, and RK performed the analyses, RK and TC wrote the manuscript, TC, ST and RK developed the Supplementary Information, SMC, ST and J-MG contributed to the research design and commented on the draft

Data accessibility statement: The data supporting the text is available here: https://figshare.com/articles/sheep_data_1986_to_1996_csv/11611911

Running title (< 45 char): Variation in life history strategies

Keywords (≤ 10): life history, *r*-selection, *K*-selection, evolution, density dependence, population dynamics, IPM, stochasticity, Soay sheep, life-history trade-offs

Document type: Letter

Word counts: abstract 153, main text 4655

Number of references: 61

Number of tables: 1

Number of figures: 5

Abstract

Fluctuating population density in stochastic environments can contribute to maintain life-history variation within populations via density-dependent selection. We used individual-based data from a population of Soay sheep to examine variation in life history strategies at high and low population density. We incorporated life-history trade-offs among survival, reproduction, and body mass growth into structured population models and found support for the prediction that different life history strategies are optimal at low and high population densities. Shorter generation times and lower asymptotic body mass were selected for in high-density environments even though heavier individuals had higher probabilities to survive and reproduce. In contrast, greater asymptotic body mass and longer generation times were optimal at low population density. If populations fluctuate between high density when resources are scarce, and low densities when they are abundant, the variation in density will generate fluctuating selection for different life history strategies, that could act to maintain life history variation.

Introduction

The idea that selection on life-history traits could vary with population density can be traced to the 1950s (Dobzhansky 1950) with *r–K* selection theory formulated by 1967 (MacArthur 1962; Wilson & MacArthur 1967). According to this within-population *r-K* selection theory, selection should favour strategies that can rapidly turn abundant resources into offspring at low population density, while at densities close to carrying capacity, strategies allowing the efficient acquisition of limiting resources should be optimal. Pianka (1970) attempted to generalize within-population theory to explain life history variation observed across distantly related species by proposing the *r-K* selection continuum. By contrasting sets of life history

traits associated with *r*- and *K* selection he proposed an axis of life history strategy variation spanning species with fast rates of turn-over such as mice to those with a slow turn-over such as elephants.

r- and *K*-selection theory and the *r*-*K* continuum became dominant paradigms in evolutionary biology before their fall from grace in the late 1970s (Stearns 1977, 1992; Reznick *et al.* 2002). Two reasons for their demise were (i) the theory could not be extended to entire life histories, and (ii) a lack of evidence for the existence of the *r*–*K* continuum from within populations (Stearns 1977; Mueller 1997; Reznick *et al.* 2002) despite support for its existence from comparative cross-species analyses (Stearns 1983; Boyce 1984; Gaillard *et al.* 1989). The emphasis of life-history evolution research primarily shifted from density-dependent selection to age-specific mortality (Stearns 1992; Reznick *et al.* 2002) and to the closely related 'pace-of-life' concept (Saether 1987; Ricklefs & Wikelski 2012).

Nowadays, there is increasing evidence of selection for traits associated with *r* and *K* life histories both across and within species. Within species, great tits (*Parus major*) that have small clutch sizes have a higher fitness at high densities than those with large clutch sizes and tend to be more *K*-selected than those at lower densities (Both *et al.* 2000; Saether *et al.* 2016). Furthermore, Trinidadian guppies (*Poecilia reticulata*) living in the absence of predators at high population densities exhibit larger adult size, mature later, and exhibit lower reproductive effort than those living with predators at lower densities (Reznick *et al.* 1990). Because guppies living without predators compete more strongly for food than those living with them, the guppies provide evidence of *r*-*K* selection theory (Reznick *et al.* 2002; Bassar *et al.* 2013).

Examples such as the Trinidadian guppies have contributed to a revival in the popularity of *r*–*K* selection within populations. Work typically focuses on characterising *r*-*K* selection theory in micro-organisms in the laboratory (e.g. Mueller 2009) or in the

development of models (e.g. Engen *et al.* 2013; Oizumi *et al.* 2016; Lande *et al.* 2017). In addition, there is recent empirical evidence for density-dependent selection on clutch size within a population of wild great tits (*Parus major*) (Saether *et al.* 2016). However, the question remains of how to extend the theory to entire life histories while identifying life-history trade-offs that can be masked within populations in the field by variation in individual quality (van Noordwijk & de Jong 1986), and to test for the maintenance of different life history strategies. Until this is achieved, our understanding of the role of density-dependent selection in moulding life histories in nature will remain rudimentary.

In natural populations, stochastic environmental factors lead population sizes to fluctuate. These fluctuations are often caused by an interaction between density dependence and stochastic environmental factors. For example, in Soay sheep (*Ovis aries*) – the focus of this paper – population declines of up to 60% occurred when population size was large and winter weather was harsh (Coulson *et al.* 2001). Such periodic changes in population size have the potential to generate fluctuating selection on life history traits. In particular, according to *r-K* selection theory, at low densities, a fast turn-over of highly productive individuals should be selected for, whereas a slow turn-over of individuals with high competitive ability to acquire resources should be favoured at high density. In turn, these periodic changes could either contribute to the maintenance of variation in life history strategies within a population, or lead to stabilizing selection around an intermediate phenotype as found by Seather *et al.* (2016).

Here we studied how fluctuating population densities of Soay sheep affects within-population variation in life history strategies using Integral Projection Models (IPMs). IPMs are structured population models which describe the expected phenotypic trait trajectories based on functions of trait-dependent demography, and consequently the entire expected life history of the group of individuals over which they are parameterized (Easterling *et al.* 2000;

Ellner *et al.* 2016). These trait-dependent functions are typically identified using linear or linearized regressions. The trait we use, body mass, is known to affect both survival and reproduction in Soay sheep, and is affected by population density (Pelletier *et al.* 2007; Coulson 2012). First, we estimated covariances across all parameters by removing each individual from the dataset in turn i.e. 'de-lifing' the dataset (Coulson *et al.* 2006). The covariance structure is then used to generate random IPMs where each IPM is defined as a set of four functions with its own unique parameterisation and represents a life history strategy. These strategies span the range of possible life history strategies we expect sheep to follow given the phenotypic life history trade-offs within and between demographic functions (see Methods). Then, we investigated the evolutionary dynamics of life histories by competing each of the randomly generated strategies against one other at a range of densities, and ranked each strategy according to fitness. Next, we identified the fittest strategies (i.e. strategies with the highest equilibrium population growth rate) at low and high density. Finally, we repeated this exercise in a stochastic environment. Our work provides a way to extend research beyond laboratory experiments to observational field studies to examine selection on life history strategies, and provides an example where density-dependent selection has the potential to be an important driver of life history evolution.

Methods

Structured Population Model including body mass – IPM

Our model is of a long-term, individual-based study of Soay sheep living on a predator free island in the St. Kilda archipelago, Scotland (Clutton-Brock & Pemberton 2004). We used a previously published IPM parametrised for this population and analysed by Coulson (2012). The model was parameterised using data of female sheep as the growth rate of the population is female-dominant (Coulson *et al.* 2001). None of the statistical models used to construct the

IPM we use from Coulson (2012) include age (see discussion). The IPM consists of four functions describing how body size z influences survival, reproduction, growth and offspring size. The survival and reproduction functions are described by generalized linear functions:

$$S(z,t) = \frac{1}{1 + \exp\left(-(s_0 + s_1 z + s_2 N_t)\right)} \quad (1)$$

$$R(z,t) = \frac{1}{1 + \exp\left(-(r_0 + r_1 z + r_2 N_t)\right)} \quad (2)$$

with z representing body mass and N_t population size at time t. The growth $G(z'|z,t)$ and parent-offspring functions $D(z'|z,t)$ are described by Gaussian probability density functions, i.e. the probability that an individual with body mass z at time t will have a body mass, or produce offspring, with body mass z' at time $t+1$:

$$G(z'|z,t) = \frac{1}{\sqrt{2\pi\sigma_g^2(z')}} \mathrm{e}^{-\frac{(z-E_g(z'))^2}{2\sigma_g^2(z')}} \quad (3)$$

$$D(z'|z,t) = \frac{1}{\sqrt{2\pi\sigma_d^2(z')}} \mathrm{e}^{-\frac{(z-E_d(z'))^2}{2\sigma_d^2(z')}} \quad (4)$$

with the function $E_g(z')$ predicting expected body mass and $E_d(z')$ predicting offspring's expected body mass at $t+1$ being linear and of the form

$$E_g(z') = \gamma_0 + \gamma_1 z + \gamma_2 N_t \quad (5)$$

$$E_d(z') = \delta_0 + \delta_1 z + \delta_2 N_t \quad (6)$$

The functions $\sigma_g^2(z')$ and $\sigma_d^2(z')$, to describe the variance around the expectation, are also linear but do not contain terms for population density

$$\sigma_g^2(z') = \gamma_3 + \gamma_4 z \quad (7)$$

$$\sigma_d^2(z') = \delta_3 + \delta_4 z \quad (8)$$

Model selection is described in Coulson (2012) and the resulting parameter values and descriptions of the parameters can be found in Table 1.

The IPM then iterates the distribution of z at t, $n(z,t)$ to $n(z',t+1)$:

$$n(z',t+1) = \int [D(z'|z,t)R(z,t) + G(z'|z,t)S(z,t)]n(z,t)dz \quad (9)$$

where population size is $N(t) = \int n(z,t)dz$. The IPM can be written as a matrix approximation as

$$\mathbf{n}(t+1) = [\mathbf{D}(t)\mathbf{R}(t) + \mathbf{G}(t)\mathbf{S}(t)]\mathbf{n}(t) \quad (10)$$

We checked if the prediction did not produce negative values for body mass and variances, which would indicate that the model is not properly parameterised.

Estimating the correlation and variance-covariance between parameters

The correlation and variance-covariance matrix across all parameters of the IPM capture trade-offs between life-history characteristics. To estimate the correlation and variance-covariance matrix, we needed to know how much each individual deviated from each of the

functions describing the population (functions 1 – 8), and correlate these deviations. We used a technique called 'de-lifing' (Coulson *et al.* 2006), which is analogous to the take-one out jack-knife. If individual *l* is taken out of the individual-based dataset, and the models re-parameterized, a new set of parameters θ^{-l} is generated. This describes the life history of the population with individual *l* removed. Then, if this new set of parameters is subtracted from the original set, $\delta^l = \theta - \theta^{-l}$, it will result in a vector which describes the contribution of individual *l* to each of the parameters. If the data set across *n* individuals consists of *m* rows where *m*>*n*, which is the case for the Soay sheep dataset, each of the *m* rows was removed sequentially and $\delta^m = \theta - \theta^{-m}$ calculated. Then $\delta^l = \frac{1}{Q}\sum \delta^m$ was calculated, where *Q* is the number of rows associated with individual *l*.

Sometimes removing an individual from the data set does not impact the statistical estimation of a function or its parameters: in such cases element *x* of θ will result in $\theta_x = \theta_x^{-l}$. For example, if an individual dies at time *t*, it will not contribute to the development function at time *t* because development is conditional on surviving. For those cases δ_x^t is undefined, and these rows were removed. For the Soay sheep dataset, of 858 unique females we retained 852 females of a total of 2529 events for the survival parameters, 858 females of a total of 2601 events for the recruitment parameters, 644 females of a total of 1367 events for the development parameters and 223 females of a total of 377 records for the mother-offspring transmission parameters. We then calculated the pairwise correlation and covariances between each pair of parameters across the δ^l sets and constructed their correlation matrix.

Prior to using the de-lifing approach we attempted to estimate the covariances between parameters using hierarchical Bayesian mixed models. In principle, parameter covariances could be estimated across posterior distributions. However, the different number of individuals available to parameterize each function made this approach problematic, as

missing values meant that trait values required imputation for growth and mother-offspring transmission for individuals that did not survive or reproduce. We consequently adopted the de-lifing approach. In Appendix S1 in the Supporting Information we demonstrate the conditions under which the de-lifing approach will give equivalent results to a mixed modelling approach when data do not need to be imputed. We are able to show that in our case, the de-lifing approach is expected to give similar estimates to the use of mixed models.

Ranking life history strategies in density-dependent deterministic environments

We used the variance-covariance matrix to generate 10,000 random parameter sets. Each parameter set *i* was used to construct an IPM describing life history strategy *i*. When density-dependent processes do not operate, equilibrium growth rate *r* is mean fitness in deterministic environments (Fisher 1930). In initial simulations, we held the population size constant at 200 individuals, close to the lowest observed population size, and calculated equilibrium growth rate *r* of each IPM. We then ranked the strategies such that the fittest strategy has the highest growth rate. For each strategy *i* we calculated carrying capacity, K_i. For each IPM at high and low density we also calculated the equilibrium size structure $\mathbf{u}_i$, generation time (Steiner *et al.* 2014), and asymptotic body mass defined at the point where the function $E_g(z)$ (eq. [5]) crossed the $z = z'$ line where expected body mass growth from time *t* to time *t+1* is zero.

When population sizes are close to carrying capacity, *r* does not represent mean fitness (Benton & Grant 2000; Sæther & Engen 2015). Instead, at high population densities, we initially identified strategy rankings using pairwise evolutionary invasion methods (Maynard-Smith 1993; see Appendix S2). We found that at high population density, carrying capacity is fitness in our linearized density-dependent deterministic model, which extends a

result from previous models of *r* and *K* selection in linear, deterministic, density-dependent models (Roughgarden 1971; Lande *et al.* 2009).

We ranked the 10,000 random life histories based on their *r* and *K*, and we plotted the functions defining the five fittest life history strategies at low and high density. To characterize these life history strategies, we calculated the mean survival rate, the mean reproductive rate, the mean and variance in offspring and adult body mass, the equilibrium population growth rate, and a metric of reproductive investment for each population size between 100 and 600 individuals. We calculated reproductive investment as the potential survival cost of reproduction by first calculating the elasticities (partial derivatives) of the population growth rate of strategy *i* at density *N*, $\lambda_i(N)$ to each element *pq* of the survival and reproduction matrices, S_{pq} and R_{pq} respectively, before summing across all *pq*s: $\sum_{pq} \frac{\partial \lambda_i(N)}{\partial S_{pq}}$ and $\sum_{pq} \frac{\partial \lambda_i(N)}{\partial R_{pq}}$. We then define reproductive investment as the ratio $\frac{\sum_{pq} \frac{\partial \lambda_i(N)}{\partial R_{pq}}}{\sum_{pq} \frac{\partial \lambda_i(N)}{\partial S_{pq}}}$ (Jones & Tuljapurkar 2015).

Stochastic IPMs

We extended our models for each strategy to stochastic environments by including random year effects in the survival, reproduction, development and mother-offspring functions (Ellner & Rees 2006). We used the random effect models fitted by Coulson (2012), see Table 1 for parameter estimates. First, we constructed a correlation and variance-covariance matrix in the same way as for the deterministic case. Then, for 100 randomly selected life history strategies (i.e. parameter sets), we ran simulations for 1200-time steps and recorded the population size at each *t*. At each time step we draw random perturbations to the intercepts of each of the four functions. For each strategy *i* we consequently generated a time series of population sizes $\mathbf{N}_i = N_i(1), N_i(2), \ldots, N_i(1200)$. To determine whether strategy *j* could

invade strategy i we ran a simulation of the dynamics of strategy j using the population sizes $\mathbf{N}_i$, recording $\mathbf{N}_{j,i}$. For time steps 201 to 1200 we calculated the long-run stochastic growth rate, a_j. If $a_j > 0$ j invaded strategy i. This approach took prohibitively long to run for all 10,000 strategies competing against each other. To identify the optimal strategy at smaller population sizes we took time series of N_is for each strategy at carrying capacity, calculated the mean, and then reduced each population size by subtracting a value x from each value such that the time series of N for each strategy had the same mean value (these mean values were 100, 200, …, 600). We then calculated the long-run stochastic growth rate for each of these values. No population size in any simulated time series dropped to 0. Strategies were ranked by their fitness at each mean population size, with fitness measured as mean asymptotic population size. In a similar manner to the deterministic case, fitness at low density is the long-run stochastic growth rate (Tuljapurkar & Orzack 1980); at high density we used mean asymptotic population size as the fitness measure.

Results

Examining covariances between parameters revealed negative relationships between the intercepts and the slopes within the survival and reproduction functions and a mixture of weaker negative and positive relationships of parameters across functions (Fig. S3.1a, b in Appendix S3). Covariances between intercepts and slopes are likely statistical artefacts that occur when the mean of x and y in regression analyses are greater than 0. In contrast, non-zero covariances across functions are consistent with life history trade-offs. However, extracting biological insight from high-dimensional correlation/(co)variance matrices such as these is difficult. Instead, we investigated the functions of the five best-ranked strategies in low and high-density environments.

As expected, at low density, the five fittest life history strategies in a low-density environment had higher survival and recruitment rates than the five strategies that are fittest in a density-dependent environment (Fig. 1ab). At high density close to *K* where density-dependence is strong, this pattern was reversed. Average body mass (Fig. 1c) and offspring body mass (Fig. 1d) both declined with increasing population density, but the functions for the fittest strategies in both low- and high-density environments overlap. The variance of adult body mass (Fig. 1e) and offspring mass (Fig. 1f) did not show a consistent pattern with population density, or with strategy. The fittest strategies at low population densities had the lowest reproductive investment relative to investment in survival in density-dependent environments, and *vice versa* (Fig. 1g). Population growth rate showed a similar pattern (Fig. 1h).

Why do these patterns occur? They arise because of a trade-off between demographic functions across changing densities. Survival and recruitment rate for a given body mass at low density does not translate to similar rates at high density. Individuals that are consequently fit at low density are unfit at high density and *vice versa*. Strategies arise that are best fitted to either high or low density, but not at both. In particular, heavier individuals always had highest survival and recruitment probabilities, but the slopes differed between population density and life history strategy (Fig. 2ab). At low population density, the life history strategy that is fittest in low-density environments includes highest survival rates for all body masses (Fig. 2a). This pattern is reversed at high population density. For recruitment the pattern is different: at low population size, lighter individuals of the fittest life history strategy in low-density environments produced more offspring than those of the fittest life history strategy in density-dependent environments (Fig. 2b), while heavier individuals of fittest life history strategies at both low and high density had a similar probability to produce recruits. At high population sizes, fittest life history strategies in both low- and high-density

environments recruited at a similar rate when individuals were light, while heavy individuals with an optimal life history strategy at high density produced more offspring. There was little variation in expected body mass development between strategies (Fig. 2c). At high population sizes expected offspring mass was lower compared to low population sizes for all adult masses, and there was little difference between optimal strategies at low and high density (Fig. 2d). Variance around the expected development and offspring body mass also did not differ between the two strategies (Fig. 2ef).

How do these differences translate into life history characteristics? Correlations of fitness (measured as equilibrium growth rate at low density and carrying capacity at high density) with generation time (Fig. 3ac) and asymptotic body mass (Fig. 3bd) at low (Fig. 3ab) and high (Fig. 3cd) density reveal that in low density there is selection for increased asymptotic body mass and longer generation times, while at high density there is competition for smaller asymptotic body mass and shorter generation times. There is substantial scatter around these associations, and in particular, selection for large body mass at low density is relatively weak.

The x-axes of fig. 3b and 3d show there is little overlap in asymptotic body mass between high and low population density suggesting that fluctuations in density generate a substantial amount of body mass plasticity. In Fig. 4 we plotted the distribution of the asymptotic body mass at low and high population density, and marked the body mass of the fittest strategy at high density in both distributions, as well as the body mass of the fittest strategy at low density in the low population density distribution. The difference in body mass between low and high population density of the fittest strategy at low density, and between low and high population density of the fittest strategy at high density, suggest that changes in average population body mass observed in the Soay sheep population are likely

almost entirely due to phenotypic plasticity rather than a change in strategy frequency (Ozgul *et al.* 2009).

If we included environmental stochasticity to allow populations to fluctuate around a mean (Fig. 5), optimal strategies at high density could only manifest themselves if the mean population size is higher than ~400 individuals (Fig. 5). In that case, the strategy at low density does not perform well, i.e. strategy rank is close to the 80^{th} percentile. When density-independent mortality is high, leading to low population sizes, the strategy at low density wins all competitions. This model reveals that at a wide range of density-dependent environments, depending on mean population density, a single (i.e. low or high density) life history dominates.

Discussion

We used a de-lifing approach (Coulson *et al.* 2006) to estimate life-history trade-offs which we included in structured population modelling followed by evolutionary invasion analyses to demonstrate evidence of density-dependent selection on life histories in Soay sheep. Our outcomes support the occurrence of *r-K* selection within populations in the wild. We found that individuals with a particular life history could not simultaneously maximise fitness for both high- and low-density environments: survival and fertility rates were higher for the fittest life history strategies in low-density environments compared to the same strategies in high-density environments. Conversely, survival and fertility rates of the fittest life history strategies in high-density environments were higher compared to the same strategies at low density. Moreover, the fittest life history strategies in low-density environments involved more investment in reproduction than survival in low density environments compared to the strategies fittest in high-density environments. As population size increases, both strategies involve increased investment in survival relative to reproduction. As expected from current

323 evolutionary theories on life history evolution (Stearns 1992), trade-offs between survival and
324 reproduction do exist across environments, which prevent individuals to be masters of all
325 trades.

326 Environments where low density strategies thrive, i.e. environments where resources
327 are not limited, are unlikely to last for long in the island population of Soay sheep examined
328 here because they exist in a predator-free environment and as such, the population can rapidly
329 increase towards carrying capacity where high-density strategies have higher fitness.
330 However, in populations where predation plays a key role in limiting population size, the
331 population could be kept well below carrying capacity thereby favouring low density life
332 histories (Reznick *et al.* 2002; Bassar *et al.* 2013). In such an environment, it is possible that
333 a set of phenotypic traits that reduce susceptibility to predation will be selected (Yoshida *et*
334 *al.* 2003), which may alter trade-offs and thereby influence life history traits such as life cycle
335 speed (Yoshida *et al.* 2003) or body size (Tollrian 1995; van Leeuwen *et al.* 2008).

336 The inferences from our deterministic modelling framework holds for stochastic
337 approaches. We found that the same processes favour either low- or high-density strategies in
338 both types of models such that, for a given stochastic environment with population densities
339 fluctuating around the mean, a single strategy dominated. When density-independent
340 processes substantially reduce survival or fertility rates, the population never reaches a
341 sufficiently large size for density-dependence to exert a brake on population growth, and low-
342 density strategies that fare badly at high densities, dominate. In contrast, when density-
343 independent processes have little effect on survival or fertility, the population attains an
344 average size where high-density strategies are evolutionary stable. This provides support for
345 theoretical modelling approaches (Engen & Saether 2017; Lande *et al.* 2017). Furthermore it
346 extends the relevance of our findings to natural situations as most animals experience
347 fluctuating environments in the wild, caused for instance by severe weather and diseases, that

impose density-independent mortality reducing population size (Boyce 1984). To maintain different life history strategies within a population in a stochastic environment, density-independent processes that influence mean population size need to alternate over multiple time steps passing a population size threshold that results in a switch between evolutionarily stable life history strategies (Fig. 5).

Long-term changes of mean population size within a stochastic environment can be caused by habitat and climate change (Simmonds & Coulson 2015; Kentie *et al.* 2018; Paniw *et al.* 2019), outbreak of diseases (Altizer *et al.* 2006), or arrival or disappearance of a new competitor or predator species (Fritts & Rodda 1998; Courchamp *et al.* 2003; Duyck *et al.* 2007). For example, the North Atlantic Oscillation influences the Soay sheep population on St. Kilda (Coulson *et al.* 2001; Pelletier *et al.* 2007) – a large-scale driver of local climate that exhibits multi-decadal oscillations and has recently experienced a multi-decadal trend towards large mean values. Mortality is increased with a positive NAO, leading to a lower mean population size (Simmonds & Coulson 2015), thereby generating fluctuations in the relative contributions of density-dependent and density-independent processes to variation in demographic rates.

Trade-offs in other life history parameters were also evident, with favoured life histories at low population densities exhibiting longer generation time and larger asymptotic body mass, whereas the opposite was true for life histories favoured at high-density environments. This finding aligns with previous work on Soay sheep demonstrating longer generation time at lower population densities (Coulson & Crawley 2004). However, generation time does not always show this pattern with population density in ungulates (Gaillard *et al.* 2005; Bjørkvoll *et al.* 2012). For instance, in contrast to Soay sheep, roe deer populations show an increase in generation time with increasing population size (Nilsen *et al.* 2009). This contrasting pattern might be explained by the between-species differences in the

interplay between density-dependent responses of survival and reproduction and potential demographic impact of these parameters. When density-dependent responses exactly match demographic elasticity patterns, generation time remains unchanged. Generation time increases if density-dependent change relative to demographic elasticity is higher in reproduction than in survival and decreases if the reversed pattern occurs.

Our model shows that the difference in body mass between optimal life histories at low and high densities can be generated from density-mediated phenotypic plasticity rather than evolution. Asymptotic body mass within a life history strategy differed more between low- and high-density environments than the difference of asymptotic body masses of the best low- and high-density strategy within an environment. Soay sheep have shrunk in size over the course of the long-term study (Ozgul *et al.* 2009), which was predominantly thought to be due to a plastic response to altered winter conditions mediated through slower growth rates of lambs. Increased population density increases competition for food and, as sheep are scramble competitors (Pérez-Barbería & Gordon 1999), reduces the energetic gain per individual thereby lowering body growth rates. Less severe winter conditions extended the grass growing season, giving lighter individuals a better chance to survive the winter, resulting in reduced average growth rates and increased population density (Ozgul *et al.* 2009).

Although our approach revealed evidence for directional selection of longer generation times at low population densities, the predicted generation times exceeded maximum life expectancy in Soay sheep. The reason for this is that we did not include age-dependence of demographic parameters, and in particular senescence, in our model (Caswell 2001; Jones *et al.* 2008). Stage- and age-structured integral projection models have been developed (Coulson *et al.* 2010; Ellner *et al.* 2016) but they include more parameters than the simple IPM we used here. The inclusion of a senescent age-class would reduce estimates of

generation time at low density, but would have increased model complexity. It is not clear in what way the inclusion of a senescent age-class would have altered our results, but this should not alter our key finding that, contrary to the standard *r-K* selection theory, generation time was longer at low than at high density. Indeed, from a life table approach including the full schedule of age-specific survival and reproduction, Coulson & Crawley (2004) did report longer generation times at low density (cohort generation time of 4.92 years vs. 2.95 at high density).

Our modelling approach provides a framework to study density-dependent selection within a natural population allowing for life-history trade-offs. Our model only considered a single trait, body mass. However, other traits influence survival and reproduction and hence carrying capacity, generation time and asymptotic body mass. If we were to extend our size-structured life history models to include other traits such as metabolic rate (Wortel *et al.* 2018) and energy budgets (Smallegange *et al.* 2017), we may expect the variance in the scatter around Fig. 3 to decline as we search for multi-trait structured life history-strategies. However, this would be challenging as model complexity would further increase while interpretation of the results becomes more challenging.

Acknowledgements

We would like to thank the Soay sheep project, all collectors of field data, and particularly Josephine Pemberton, Tim Clutton-Brock and Loeske Kruuk. RK was funded by the Royal Society.

References

Altizer, S., Dobson, A., Hosseini, P., Hudson, P., Pascual, M. & Rohani, P. (2006). Seasonality and the dynamics of infectious diseases. *Ecol. Lett.*, 9, 467-484.

Bassar, R.D., Lopez-Sepulcre, A., Reznick, D.N. & Travis, J. (2013). Experimental evidence for density-dependent regulation and selection on Trinidadian guppy life histories. *Am. Nat.*, 181, 25-38.

Benton, T. & Grant, A. (2000). Evolutionary fitness in ecology: comparing measures of fitness in stochastic, density-dependent environments. *Evol. Ecol. Res.*, 2, 769-789.

Bjørkvoll, E., Grotan, V., Aanes, S., Saether, B.E., Engen, S. & Aanes, R. (2012). Stochastic population dynamics and life-history variation in marine fish species. *Am. Nat.*, 180, 372-387.

Both, C., Tinbergen, J.M. & Visser, M.E. (2000). Adaptive density dependence of avian clutch size. *Ecology*, 81, 3391-3403.

Boyce, M.S. (1984). Restitution of *r*-and *K*-selection as a model of density-dependent natural selection. *Annu. Rev. Ecol. Syst.*, 15, 427-447.

Caswell, H. (2001). *Matrix population models: construction, analysis, and interpretation*. Sinauer Associates.

Clutton-Brock, T.H. & Pemberton, J.M. (2004). *Soay sheep: dynamics and selection in an island population*. Cambridge University Press, Cambridge, UK.

Coulson, T. (2012). Integral projections models, their construction and use in posing hypotheses in ecology. *Oikos*, 121, 1337-1350.

Coulson, T., Benton, T.G., Lundberg, P., Dall, S.R.X., Kendall, B.E. & Gaillard, J.-M. (2006). Estimating individual contributions to population growth: evolutionary fitness in ecological time. *P. R. Soc. B*, 273, 547-555.

444 Coulson, T., Catchpole, E.A., Albon, S.D., Morgan, B.J.T., Pemberton, J.M., Clutton-Brock,
445 T.H. *et al.* (2001). Age, sex, density, winter weather, and population crashes in Soay
446 sheep. *Science*, 292, 1528-1531.
447 Coulson, T. & Crawley, M.J. (2004). How average life tables can mislead. In: *Soay sheep.*
448 *Dynamics and selection in an island population* (eds. Clutton-Brock, T & Pemberton,
449 J). Cambridge University Press Cambridge.
450 Coulson, T., Tuljapurkar, S. & Childs, D.Z. (2010). Using evolutionary demography to link
451 life history theory, quantitative genetics and population ecology. *J. Anim. Ecol.*, 79,
452 1226-1240.
453 Courchamp, F., Chapuis, J.L. & Pascal, M. (2003). Mammal invaders on islands: impact,
454 control and control impact. *Biol. Rev.*, 78, 347-383.
455 Dobzhansky, T. (1950). Evolution in the tropics. *Am. Sci.*, 38, 208-221.
456 Duyck, P.-F., David, P. & Quilici, S. (2007). Can more *K*-selected species be better invaders?
457 A case study of fruit flies in La Réunion. *Divers. Distrib.*, 13, 535-543.
458 Easterling, M.R., Ellner, S.P. & Dixon, P.M. (2000). Size-specific sensitivity: applying a new
459 structured population model. *Ecology*, 81, 694-708.
460 Ellner, S.P., Childs, D.Z. & Rees, M. (2016). *Data-driven modelling of structured*
461 *populations*. Springer, Charn, Switzerland.
462 Ellner, S.P. & Rees, M. (2006). Integral projection models for species with complex
463 demography. *Am. Nat.*, 167, 410-428.
464 Engen, S., Lande, R. & Saether, B.E. (2013). A quantitative genetic model of *r*- and *K*-
465 selection in a fluctuating population. *Am. Nat.*, 181, 725-736.
466 Engen, S. & Saether, B.E. (2017). *r*- and *K*-selection in fluctuating populations is determined
467 by the evolutionary trade-off between two fitness measures: Growth rate and lifetime
468 reproductive success. *Evolution*, 71, 167-173.

Fisher, R.A. (1930). *The genetic theory of natural selection*. Oxford University Press, Oxford.

Fritts, T.H. & Rodda, G.H. (1998). The role of introduced species in the degradation of island ecosystems: A case history of Guam. *Annu. Rev. Ecol. Syst.*, 29, 113-140.

Gaillard, J.-M., Pontier, D., Allainé, D., Lebreton, J.D., Trouvilliez, J. & Clobert, J. (1989). An analysis of demographic tactics in birds and mammals. *Oikos*, 56, 59-76.

Gaillard, J.-M., Yoccoz, N.G., Lebreton, J.-D., Bonenfant, C., Devillard, S., Loison, A. *et al.* (2005). Generation time: a reliable metric to measure life-history variation among mammalian populations. *Am. Nat.*, 166, 119-123.

Jones, J.H. & Tuljapurkar, S. (2015). Measuring selective constraint on fertility in human life histories. *P. Natl. Acad. Sci. U.S.A.*, 112, 8982-8986.

Jones, O.R., Gaillard, J.-M., Tuljapurkar, S., Alho, J.S., Armitage, K.B., Becker, P.H. *et al.* (2008). Senescence rates are determined by ranking on the fast-slow life-history continuum. *Ecol. Lett.*, 11, 664-673.

Kentie, R., Coulson, T., Hooijmeijer, J.C.E.W., Howison, R.A., Loonstra, A.H.J., Verhoeven, M.A. *et al.* (2018). Warming springs and habitat alteration interact to impact timing of breeding and population dynamics in a migratory bird. *Glob. Change Biol.*, 24, 5292-5303.

Lande, R., Engen, S. & Saether, B.E. (2009). An evolutionary maximum principle for density-dependent population dynamics in a fluctuating environment. *Philos. Trans. R. Soc. Lond. B Biol. Sci.*, 364, 1511-1518.

Lande, R., Engen, S. & Saether, B.E. (2017). Evolution of stochastic demography with life history tradeoffs in density-dependent age-structured populations. *P. Natl. Acad. Sci. U.S.A.*, 114, 11582-11590.

MacArthur, R.H. (1962). Some generalized theorems of natural selection. *P. Natl. Acad. Sci. U.S.A.*, 48, 1893-1897.

Maynard-Smith, J. (1993). *The theory of evolution*. Cambridge University Press, Cambridge, UK.

Mueller, L.D. (1997). Theoretical and empirical examination of density-dependent selection. *Annu. Rev. Ecol. Syst.*, 28, 269-288.

Mueller, L.D. (2009). Fitness, demography, and population dynamics in laboratory experiments. In: *Experimental evolution: concepts, methods, and applications of selection experiments.* (eds. Garland, T & Rose, MR). University of California Press Berkeley, pp. 197-216.

Nilsen, E.B., Gaillard, J.M., Andersen, R., Odden, J., Delorme, D., van Laere, G. *et al.* (2009). A slow life in hell or a fast life in heaven: demographic analyses of contrasting roe deer populations. *J. Anim. Ecol.*, 78, 585-594.

Oizumi, R., Kuniya, T. & Enatsu, Y. (2016). Reconsideration of *r/K* selection theory using stochastic control theory and nonlinear structured population models. *PLoS ONE*, 11, e0157715.

Ozgul, A., Tuljapurkar, S., Benton, T.G., Pemberton, J.M., Clutton-Brock, T.H. & Coulson, T. (2009). The dynamics of phenotypic change and the shrinking sheep of St. Kilda. *Science*, 325, 464-467.

Paniw, M., Maag, N., Cozzi, G., Clutton-Brock, T. & Ozgul, A. (2019). Life history repsonses of meerkats to seasonal changes in extreme environments. *Science*, 363, 631-635.

Pelletier, F., Clutton-Brock, T., Pemberton, J., Tuljapurkar, S. & Coulson, T. (2007). The evolutionary demography of ecological change: Linking trait variation and population growth. *Science*, 315, 1571-1574.

518 Pérez-Barbería, F.J. & Gordon, I.J. (1999). Body size dimorphism and sexual segregation in
519 polygynous ungulates: an experimental test with Soay sheep. *Oecologia*, 120, 258-
520 267.
521 Pianka, E.R. (1970). On *r*-and *K*-selection. *Am. Nat.*, 104, 592-597.
522 Reznick, D., Bryant, M.J. & Bashey, F. (2002). *r* ‐ and *K* ‐ selection revisited: the role of
523 population regulation in life ‐ history evolution. *Ecology*, 83, 1509-1520.
524 Reznick, D.A., Bryga, H. & Endler, J.A. (1990). Experimentally induced life-history
525 evolution in a natural population. *Nature*, 346, 357-359.
526 Ricklefs, R.E. & Wikelski, M. (2002). The physiology/life history nexus. *Trends Ecol. Evol.*,
527 17, 462-468.
528 Roughgarden, J. (1971). Density ‐ dependent natural selection. *Ecology*, 52, 453-468.
529 Sæther, B.-E. (1987). The influence of body weight on the covariation between reproductive
530 traits in European birds. *Oikos*, 48, 79-88.
531 Sæther, B.-E. & Engen, S. (2015). The concept of fitness in fluctuating environments. *Trends*
532 *Ecol. Evol.*, 30, 273-281.
533 Saether, B.E., Visser, M.E., Grotan, V. & Engen, S. (2016). Evidence for *r*- and *K*-selection
534 in a wild bird population: a reciprocal link between ecology and evolution. *P. R. Soc.*
535 *B*, 283.
536 Simmonds, E.G. & Coulson, T. (2015). Analysis of phenotypic change in relation to climatic
537 drivers in a population of Soay sheep *Ovis aries*. *Oikos*, 124, 543-552.
538 Smallegange, I.M., Caswell, H., Toorians, M.E.M. & de Roos, A.M. (2017). Mechanistic
539 description of population dynamics using dynamic energy budget theory incorporated
540 into integral projection models. *Methods Ecol. Evol.*, 8, 146-154.
541 Stearns, S.C. (1977). The evolution of life history traits: a critique of the theory and a review
542 of the data. *Annu. Rev. Ecol. Syst.*, 8, 145-171.

543 Stearns, S.C. (1983). The influence of size and phylogeny on patterns of covariation among
544 life-history traits in the mammals. *Oikos*, 41, 173-187.
545 Stearns, S.C. (1992). *The evolution of life histories*. Oxford Univeristy Press, Oxford.
546 Steiner, U.K., Tuljapurkar, S. & Coulson, T. (2014). Generation time, net reproductive rate,
547 and growth in stage-age-structured populations. *Am. Nat.*, 183, 771-783.
548 Tollrian, R. (1995). Predator‐induced morphological defenses: costs, life history shifts, and
549 maternal effects in *Daphnia pulex*. *Ecology*, 76, 1691-1705.
550 Tuljapurkar, S. & Orzack, S.H. (1980). Population dynamics in variable environments I.
551 Long-run growth rates and extinction. *Theoretical Population Biology*, 18, 314-342.
552 van Leeuwen, A., de Roos, A.M. & Persson, L. (2008). How cod shapes its world. *J. Sea*
553 *Res.*, 60, 89-104.
554 van Noordwijk, A.J. & de Jong, G. (1986). Acquisition and allocation of resources: their
555 influence on variation in life history tactics. *The American Naturalist*, 128, 137-142.
556 Wilson, E.O. & MacArthur, R.H. (1967). *The theory of island biogeography*. Princeton
557 University Press, Princeton, New Jersey, USA.
558 Wortel, M.T., Noor, E., Ferris, M., Bruggeman, F.J. & Liebermeister, W. (2018). Metabolic
559 enzyme cost explains variable trade-offs between microbial growth rate and yield.
560 *PLoS computational biology*, 14, e1006010-e1006010.
561 Yoshida, T., Jones, L.E., Ellner, S.P., Fussmann, G.F. & Hairston Jr, N.G. (2003). Rapid
562 evolution drives ecological dynamics in a predator–prey system. *Nature*, 424, 303.
563
564

Table

Table 1. Parameter values used from deterministic and stochastic IPMs parameterized by Coulson (2012). Stochastic IPMs makes use of yearly random effects in each function. We report the standard deviation of the distribution of the random effect of year.

Parameter	Deterministic model	Stochastic model	Description
s_0	-0.2392	0.5807	Survival: intercept
s_1	0.1775	0.2128	Survival: slope body mass
s_2	-0.0043	-0.0074	Survival: slope population size
$\varphi_s(0, \sigma_s)$		0.9372	Survival: yearly random effect
r_0	-1.7839	-1.9421	Recruitment: intercept
r_1	0.1090	0.1112	Recruitment: slope body mass
r_2	-0.0032	-0.0030	Recruitment: slope population density
$\varphi_r(0, \sigma_r)$		0.2824	Recruitment: yearly random effect
γ_0	10.6032	11.0853	Development, mean: intercept
γ_1	0.6049	0.6032	Development, mean: slope body mass
γ_2	-0.0026	-0.0037	Development, mean: slope population size
$\varphi_\gamma(0, \sigma_\gamma)$		0.4245	Development, mean: yearly random effect
γ_3	3.7114	3.6716	Development, variance: intercept
γ_4	-0.0161	-0.0214	Development, variance: slope body mass
$\varphi_{\gamma v}(0, \sigma_{\gamma v})$		1.574	Development, variance: yearly random effect
δ_0	9.8065	11.0003	Inheritance, mean: intercept
δ_1	0.2544	0.2277	Inheritance, mean: slope body mass
δ_2	-0.0069	-0.0081	Inheritance, mean: slope population size
$\varphi_\delta(0, \sigma_\delta)$		0.7428	Inheritance, mean: yearly random effect
δ_3	8.7540	7.3228	Inheritance, variance: intercept
δ_4	-0.1219	-0.0823	Inheritance, variance: slope body mass
$\varphi_{\delta v}(0, \sigma_{\delta v})$		0.0001	Inheritance, variance: yearly random effect

Figure legends

Figure 1. How survival (a), fertility (b), expected development (c,e), expected mother-offspring relationship (d,f), reproductive investment (g) and log population growth (h) vary with population density in the fittest low density (blue) and high density (red) life histories (solid lines) and the next four fittest life histories at low and high density (dotted lines). Each association is evaluated at the mean body mass of each strategy. The vertical dotted line at the population size of 400 individuals is approximate population size of the Soay sheep population over the period the model was parameterised (see Coulson 2012).

Figure 2. Relationship between body mass and survival (a), fertility (b), expected growth (c), expected mother-offspring relationship (d) at low population size of 200 individuals (orange lines) and at high population size of 600 individuals (light blue lines). Each of the 10,000 orange and blue lines represent one strategy. The blue thick lines represent the best low-density life history strategy, the red thick lines represent the best high-density life history; solid at low population density, dashed at high population density. The variance around the expected growth (e), and variance around the expected mother-offspring relationship (f) are not density dependent and are therefore coloured grey.

Figure 3. Correlation between generation time with carrying capacity (a) and population growth rate lambda (c) and asymptotic body mass (b, d) at low (a, b) and high (c,d) density. Each point represents a strategy; green lines represent smooth loess curves. At low density the slopes of the regression lines are positive (a, b), indicating selection for a longer generation time and a large body size. The converse is true at high density (c,d).

Figure 4. Density plots of the distribution of asymptotic body mass at low (blue) and high (orange) population density. The blue and red vertical lines represent the location in the distribution of the fittest low- and high-density strategies, respectively. The red dashed vertical line represents the asymptotic body mass of the fittest high-density strategy in a low-density environment. Note that to reduce clutter, the location of the fittest low-density strategy is not marked in the distribution of asymptotic body masses at high population density. The horizontal black line represents the difference in asymptotic body mass between the fittest high-density strategy at low and high population density. The grey line represents the difference in asymptotic body mass between the fittest low- and high-density strategies at low population density. Because the black line is longer than the grey line this suggests that observed changes in body mass in the Soay sheep population are likely due to density-mediated phenotypic plasticity rather than evolution.

Figure 5. Population dynamics of low-density strategies and high-density strategies in stochastic environments. The figure on the left shows the population dynamic of the best low-density strategy (red line; mean population size was kept below carrying capacity mimicking density-independent mortality) and the best high-density strategy (red line).

610 Figure 1:

611

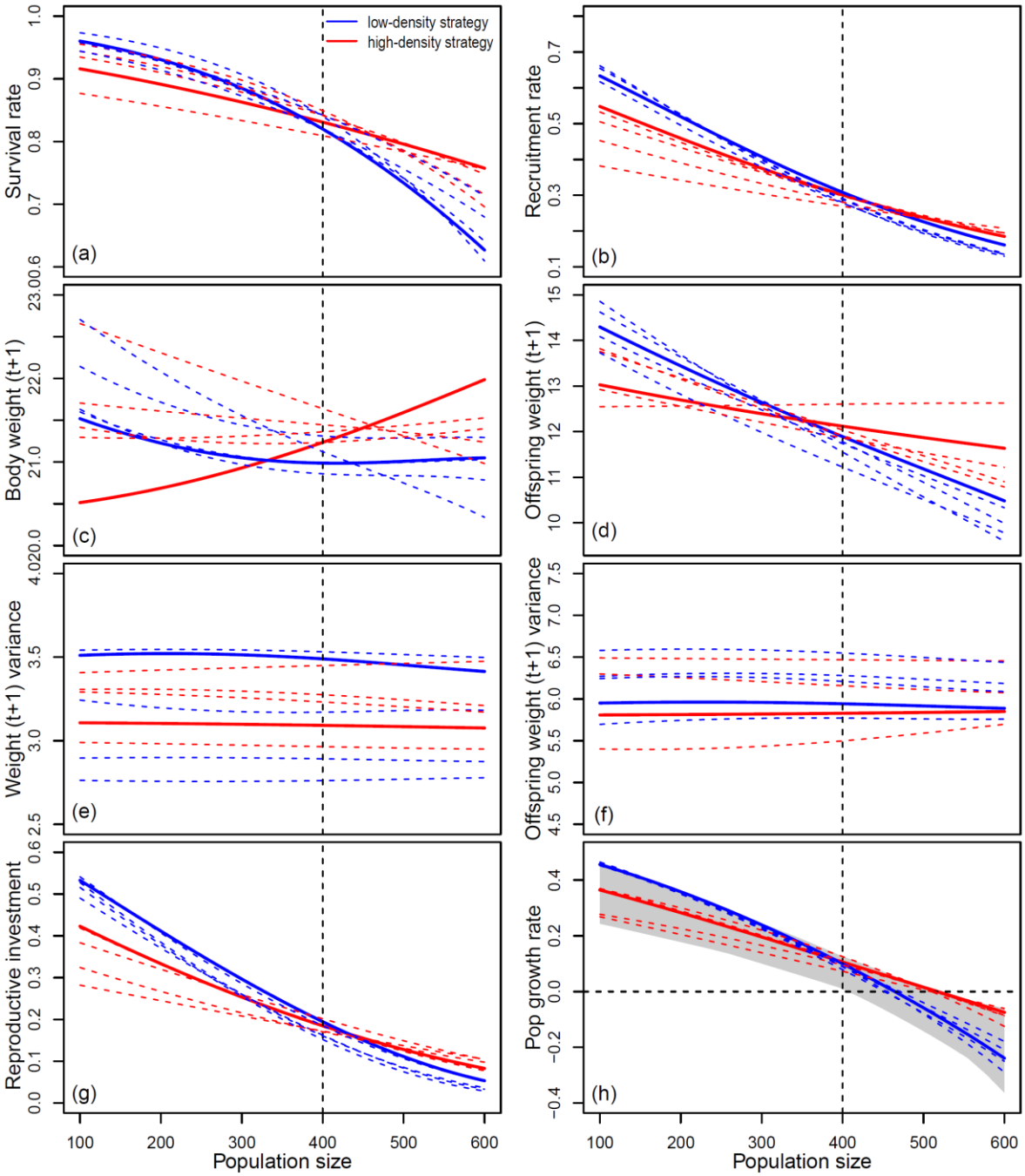

612

613

614 Figure 2:

615

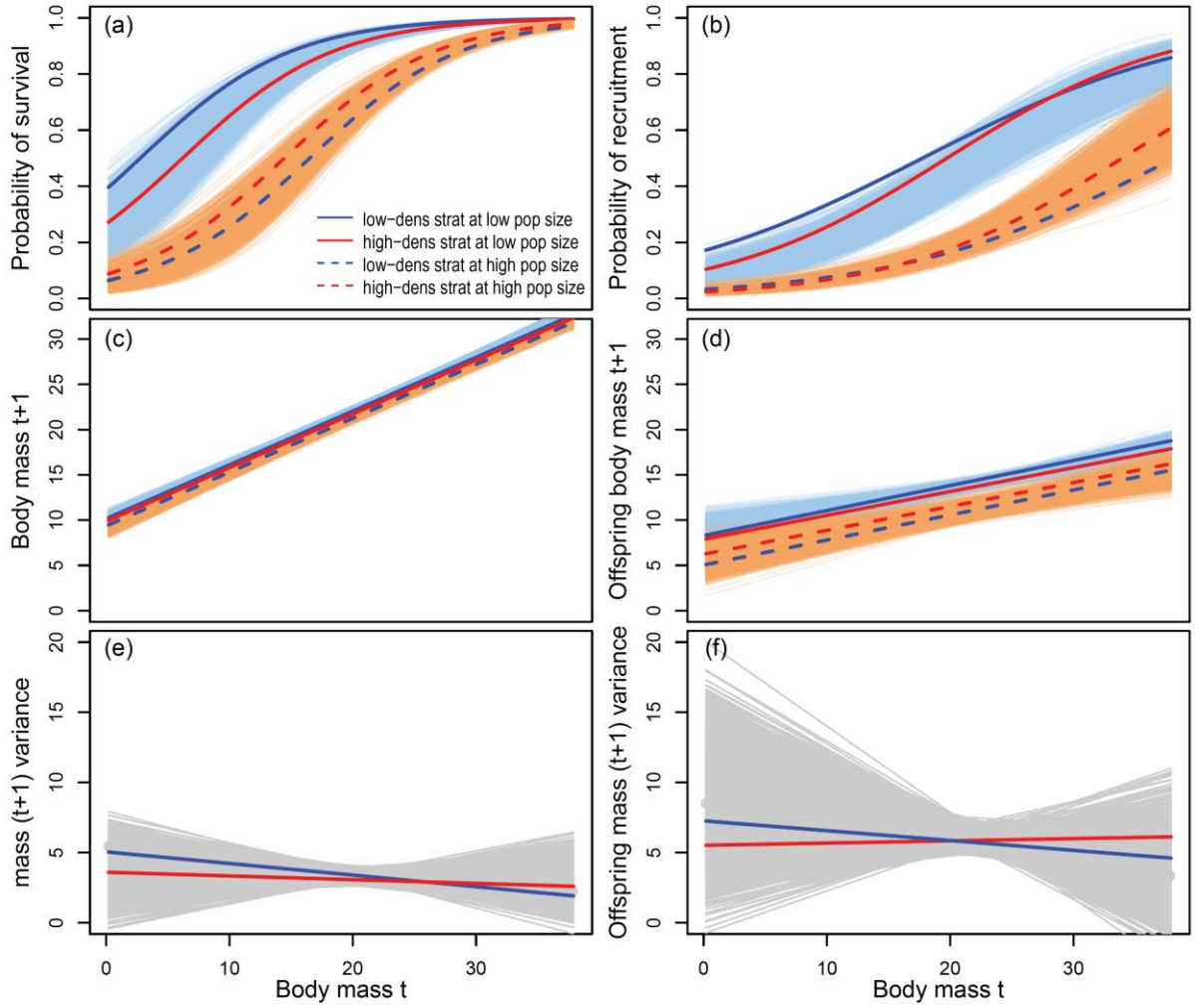

616

617 Figure 3.

618

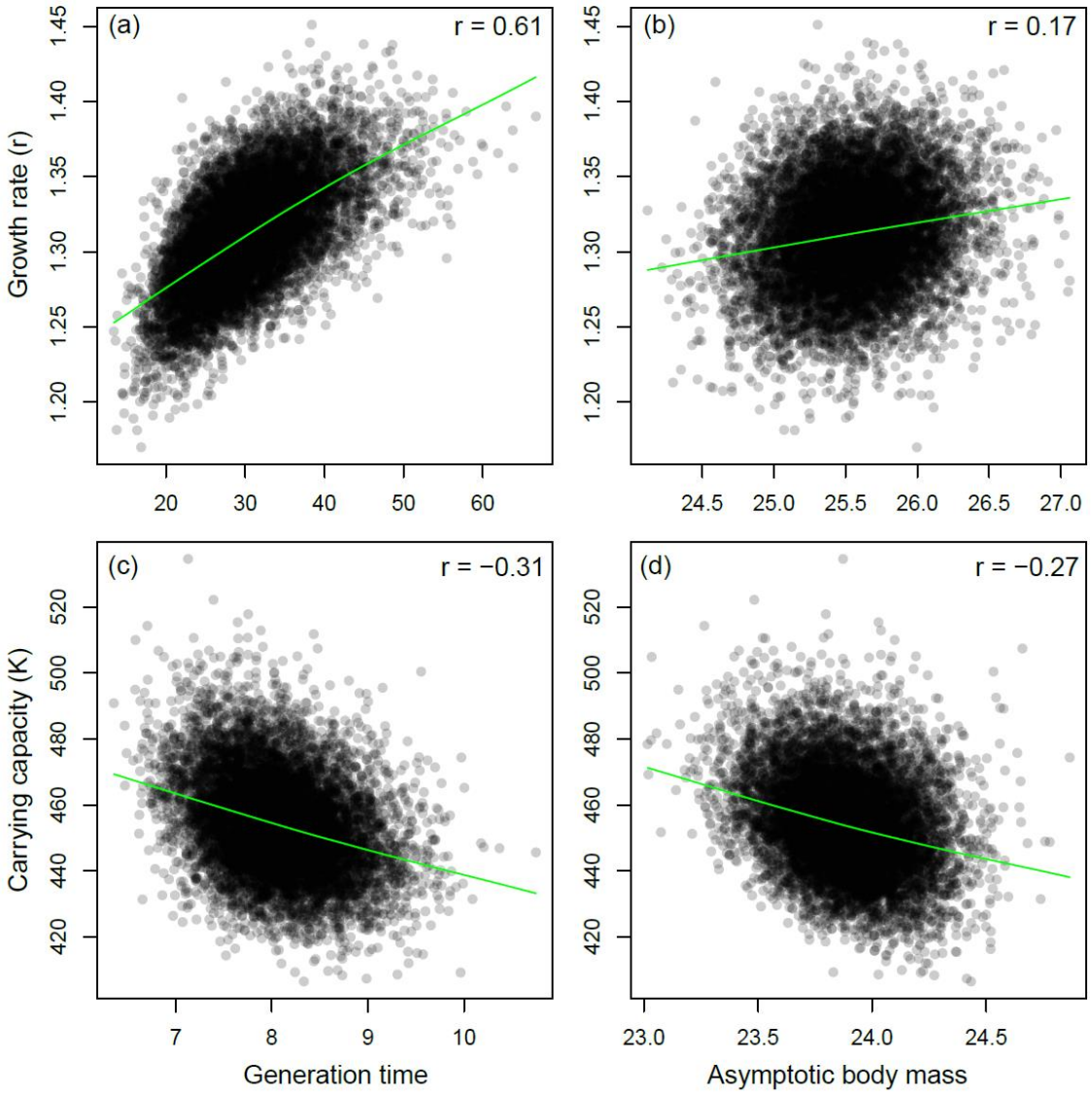

619

620

621

622

623 Figure 4.

624

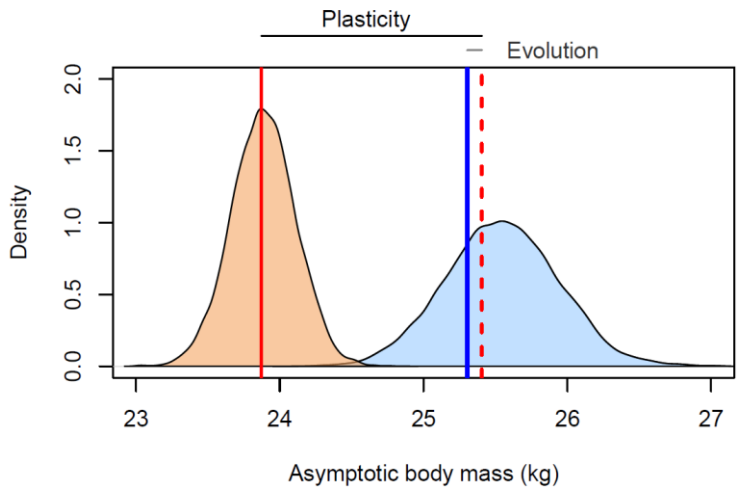

625

626

627

628 Figure 5:

629

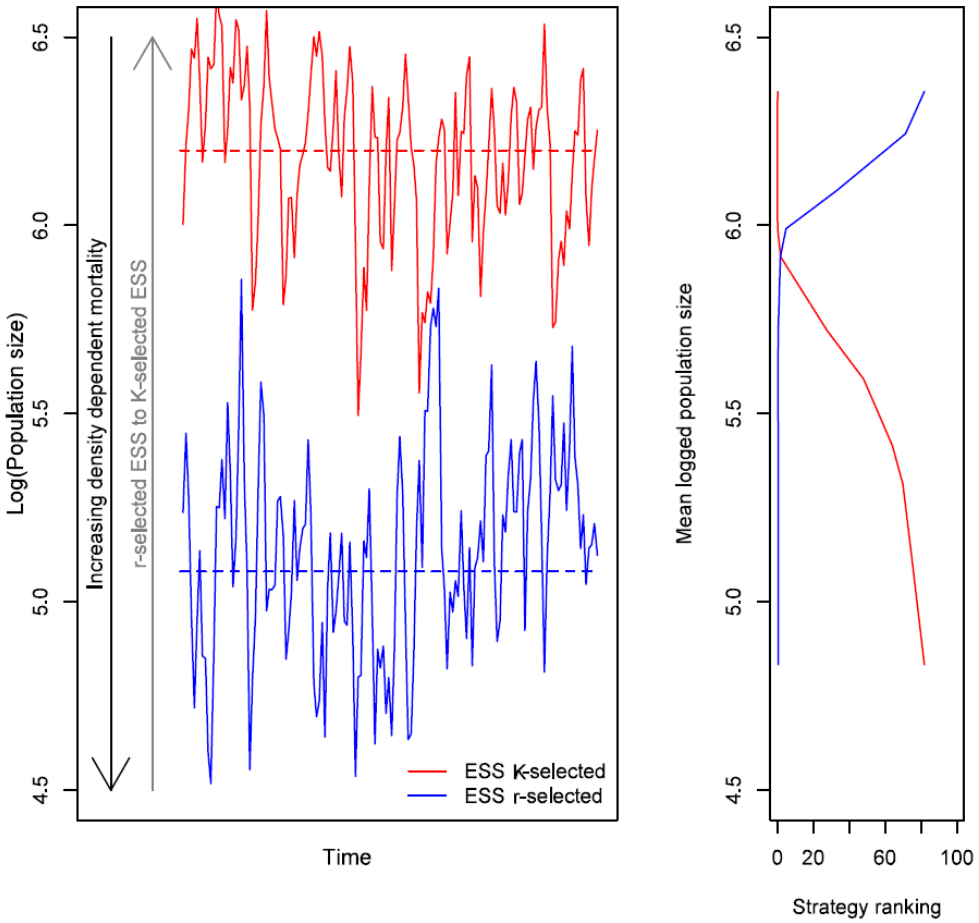

630

631

632

Supporting Information

Appendix S1. Comparing the correlation and variance-covariance matrix using the de-lifing method and using hierarchical Bayesian models

We attempted to estimate the correlation and covariance matrices between model parameters by fitting generalized linear mixed effect models with individual effects on each intercept and slope using multi-response models in the package MCMCglmm (Hadfield 2010). There were two reasons why this approach did not work. First, if an individual dies it also fails to reproduce and there it cannot contribute to the growth and inheritance function. Multi-response models as implemented in MCMCglmm impute missing data. We do not wish to impute missing data for growth rates between t and t + 1 for individuals that died during that period, or offspring body sizes for individuals that failed to breed as growth is conditional on survival and inheritance is conditional on reproduction. Second, when only a single measure exists on an individual within the data set, a BLUP for a slope cannot be estimated for that individual. We have some cases where an individual appears only once in the data set, for example if it dies aged 1. Despite the fact that we are unable to estimate the variance-covariance matrix using mixed effect models, we were interested in any correspondence between the mixed effect approach and the delifing (or take-one-out) approach (Coulson *et al.* 2006) we used. We used a mathematical approach and simulated data to examine the similarities.

Simple model

Take a very simple linear mixed model for a trait value y with balanced design,

$$\overline{y_{iJ}} = \mu + \gamma_i + \epsilon_{ij} \quad (1)$$

where we measure values on individuals $i = 1, \ldots, n$ and for ever individual we have $j = 1, \ldots, k$ measurements. The grand mean is μ, the individual random effect is γ_i which are assumed normal with mean 0 and variance V, and all other random variation is given by the ϵ_{ij} that are independent of the γ_i and that are assumed normal with mean 0 and variance V_e.

From the data, we estimate the individual means,

$$\overline{y_{i\cdot}} = \frac{1}{k}\sum_j y_{ij} \quad (2)$$

and the grand mean

$$\bar{y}_{..} = \frac{1}{n}\sum_{i} y_i \tag{3}$$

Standard methods (Searle & McCulloch 2001) show that $y_{..}$ is the BLUE for μ whereas the BLUPS for the random effects (via MLE) are

$$\gamma_i = \left(\frac{kV}{kV + V_e}\right) \tag{4}$$

As Searle and McCulloch (2001) point out, the only information in the data that tell us about γ_i are contained in the individual means $\overline{y_i}$.
Now define the delifed means

$$\bar{y}_{(-i)} = \left(\frac{1}{n-1}\right)\sum_{m \neq i} \bar{y}_{m.} \tag{5}$$

From this we have

$$\bar{y}_i = n\bar{y}_{..} - (n-1)\bar{y}_{(-i)} = (n-1)[\bar{y}_{..} - \bar{y}_{(-i)}] + \bar{y}_{..}$$

and hence the BLUPS in (4) can be rewritten as

$$\beta_i = \left(\frac{k(n-1)V}{kV + V_e}\right)\bar{y}_{..} - \bar{y}_{(-i)} \tag{6}$$

For each individual i the last term on the right above is exactly the delifed difference that Coulson computes, so we have shown that these are directly proportional to the BLUPS.

Mixed Model

A more general mixed model for a trait value y with mixed effects is

$$y_{ij} = \mu + \beta x_i + \gamma_i + \epsilon_{ij} \tag{7}$$

where the x_i are measured fixed values for individuals $i = 1, \ldots, n$. As
(Searle & McCulloch 2001) point out, the estimation of random effects can be dealt with by first estimating β and then focusing on the variables ($y_{ij} - \beta x_i$ which have a probability structure essentially the same as for the y_{ij} in (1). Hence we can expect that here too the BLUPS will be proportional to the delifed differences.

Simulation 1

We randomly generated 20 individuals each with between 2 and 20 repeated measures on a random variate, y. The number of repeated measures was generated by drawing a single random integer from a uniform distribution bounded between 2 and 20. Each individual's repeated measures were drawn from a normal distribution. Each individual's distribution had a unique mean but the same variance. The unique mean was drawn from a uniform distribution with a mean of 0 and a variance of 2. From this data set we fitted a generalised linear mixed effect model with a common intercept and individual fitted as a random effect using the R library MCMCglmm and the command lme. We extracted the BLUPs.

Next, we calculated the overall mean of y, $\bar{y}$. We then removed each individual i in turn and calculated $\delta^i = \bar{y} - \bar{y^i}$ (Coulson *et al.* 2006). We then correlated the δ^i's against the BLUPs. We repeated this exercise 1000 times. There was always a perfect correlation between the BLUPs and the δ^i's (Fig. S1.1).

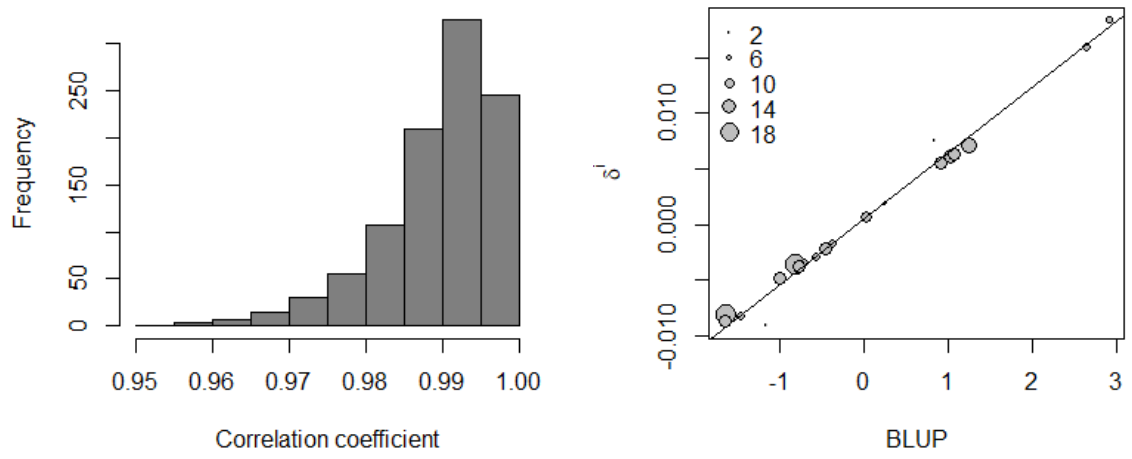

Figure S1.1. Left: histogram of correlation coefficient between the BLUP and δ^i for 1000 simulations. Right: example of correlation between BLUP and δ^i of one of the 1000 simulations. The size of the circle represents the number of repeated measures per individual.

Simulation 2

We conducted a similar exercise, except we now include a common slope. The number of individuals, and the distribution of repeated measures, were the same as in simulation 1, except that the variance is 0.2. We start by randomly determining the number of repeated measures, n, on an individual. Second, we randomly determine each individual's random intercept, a_i. Third, we generate n random values of a variate x from a normal distribution common to all individuals. Fourth, for each value in x we generate a single random variate y from the multivariate normal distribution with a mean $\beta x + a_i$ where β is a variate common to all individuals. Note that all variance in y other than that attributable to x is due to individual heterogeneity – there is no variance attributable to other factors.

From this data set we fitted a linear mixed effect model of y with x fitted as a fixed effect and individual identity fitted as random intercepts. We also removed each individual in turn and used these to estimate a^{-i} for each individual. We then correlated the individual level BLUPs against the $a^{-i}{}'s$. We repeated this exercise 1000 times. We also fitted a linear model to the entire data set and saved the fixed effect estimates.

The correlation between the BLUPs and the de-lifed a^{-i} was always high: out of 1000 simulations we found that the correlation for the BLUPs and the individual contributions to the intercept had a mean correlation of r = 0.9994 range 0.9925; 0.9999 (Fig. S1.2).

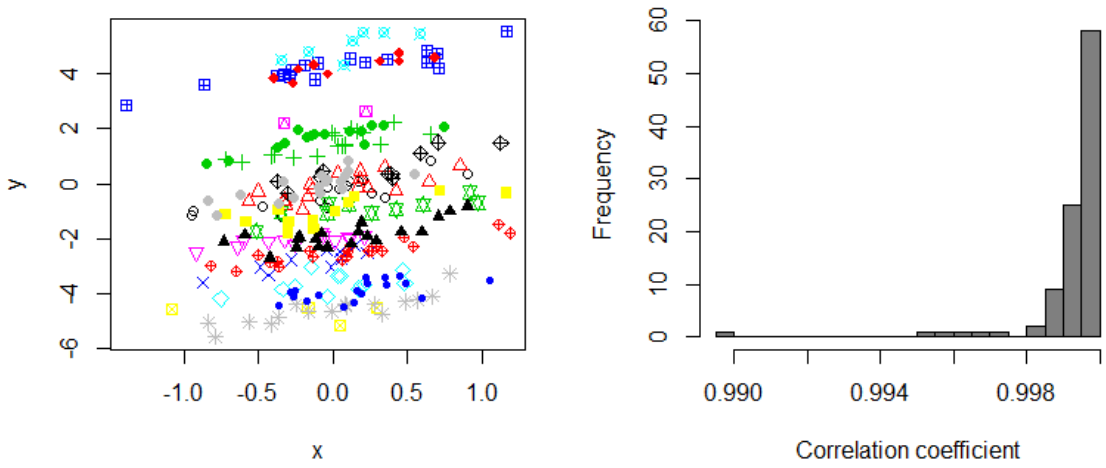

Figure S1.2. Left: one of the 1000 simulations of 20 individuals (different colours and symbols) with random intercept and common slope. Right: histogram of correlation coefficients between de-lifed means and BLUPs estimated from a linear mixed effect model with individual identity fitted as a random intercept.

Appendix S2. Outcome of strategy ranking using evolutionary invasion methods at high population density

When population sizes are close to carrying capacity, *r* does not represent mean fitness. Instead, at high population densities, we identified strategy rankings using evolutionary invasion methods. We did this with a smaller subset of 2000 randomly chosen IPMs, due to the long computation time of competing each strategy with each other strategy. For each strategy within this subset, *i*, we ran a simulation until the population dynamics converged at an equilibrium population size, K_i and structure u_i. To evaluate whether strategy *j* could invade strategy *i*, K_i was inserted in the transition matrix,

$$\mathrm{A}_j(K_i) = \mathrm{D}_j(K_i)\mathrm{R}_j(K_i) + \mathrm{G}_j(K_i)\mathrm{S}_j(K_i).$$

We then calculated the dominant eigenvalue, $\lambda_{\mathrm{j,i}}$ of the $\mathrm{A}_j(K_i)$. If $\log(\lambda_{\mathrm{j,i}}) > 0$ then strategy *j* can invade strategy *i*. Each strategy was ranked by the number of competitions they won. This smaller subset showed a precise relationship of the number of outcomes won and carrying capacity K_i (Fig. S2.1).

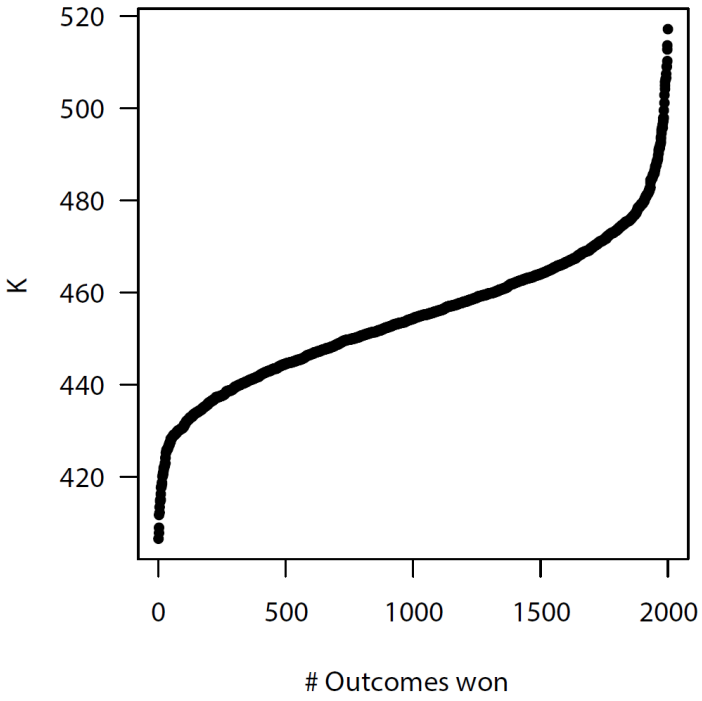

Figure S2.1. Association between strategy fitness determined by evolutionary invasion and strategy carrying capacity, *K*. We used a subset of 2000 random strategies due to computation time. Rankings by number of games won and carrying capacity are perfectly correlated.

Kentie R., Clegg S.M., Tuljapurkar S, Gaillard J-M & Coulson T. Evidence for coexisting r- and K-selected life history strategies within a population fluctuating in density

Appendix S3. Capturing trade-offs in correlation and variance-covariance matrix across all parameters of the IPM

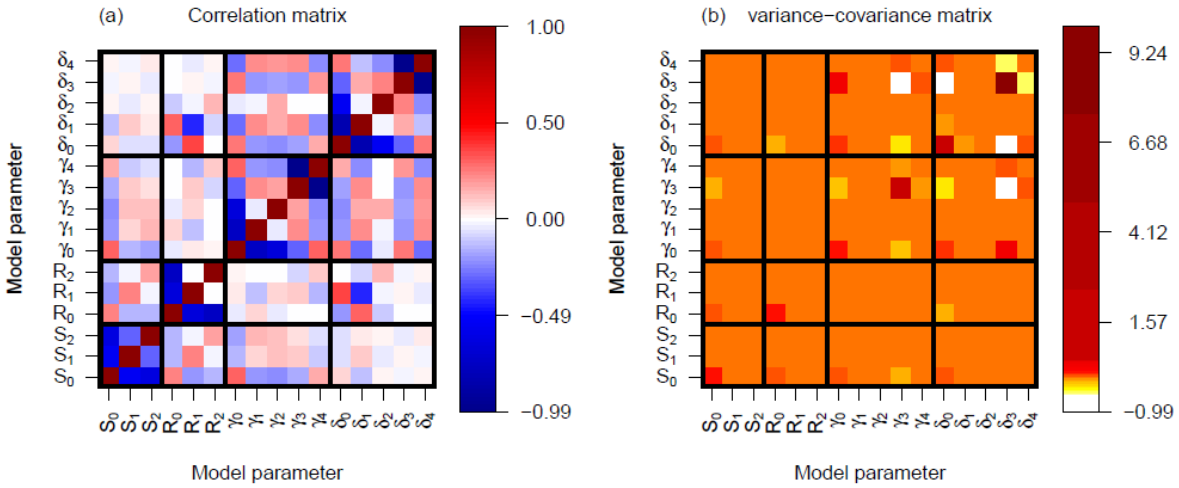

Figure S3.1. Correlation (a) and variance-covariance (b) matrices between the 16 parameters that constitute the IPM. See Table 1 in the main text for descriptions of the model parameters.

Cited literature in Appendix

Coulson, T., Benton, T.G., Lundberg, P., Dall, S.R.X., Kendall, B.E. & Gaillard, J.-M. (2006). Estimating individual contributions to population growth: evolutionary fitness in ecological time. *P. R. Soc. B*, 273, 547-555.

Hadfield, J. (2010). MCMC methods for multi-response generalized linear mixed models: the MCMCglmm R package. *Journal of statistical software*, 33, 1-22.

Searle, S.R. & McCulloch, C.E. (2001). *Generalized, linear, and mixed models*. John Wiley & Sons, New York.